

Spin Polarized Electron Scattering by Ferromagnetic Amorphous Surfaces^{*}

by

Sheng-Wei Wang

Stanford Linear Accelerator Center
Stanford University
Stanford, CA 94305

and

Materials and Molecular Research Division
Lawrence Berkeley Laboratory
and
Department of Chemistry
University of California
Berkeley, CA 94720^{**}

ABSTRACT

It is shown that kinematic atomic scattering is the predominant mechanism for the elastic backward scattering of electrons from the ferromagnetic glass $\text{Fe}_{40}\text{Ni}_{40}\text{B}_{20}$ as opposed to the resonance model recently suggested by R. K. Nesbet. The spin dependence of this scattering was determined theoretically (in the energy range below 300 eV) using various spin polarized potentials for Fe and Ni. Below 30 eV, current exchange correlation models fail to explain the experimental data even when allowing for a spin dependence in the attenuation of electrons.

(Submitted to Physical Review Letters)

* Work supported most by Department of Energy under Contract DE-AC03-76SF00515 and in part by DE-AC03-76SF00098.

** Present address: Department of Chemistry, University of California Berkeley, CA 94720

Scattering of slow spin polarized electrons from magnetic surfaces emerged recently as one of the most promising techniques to study surface magnetism¹⁻⁴. The surface magnetism can be detected by measuring the scattering asymmetry factor S defined as $S = \frac{I^+ - I^-}{I^+ + I^-}$, in which I^+ and I^- are the scattered intensities of the incident electrons having spin directions polarized parallel or antiparallel to the majority spin of the sample. A comparison of the dependence of S on the incident electron energy E between magnetic single crystal surfaces and amorphous surfaces appears to be very interesting. Wang³ has shown that S - E curves for single crystal surfaces show rich structures due to a superposition of low energy electron diffraction with the structures due to surface magnetism whereas Schilling and Webb⁵ have shown that in the case of electron scattering from liquid Hg⁵ the intensity due to atomic scattering can be separated from the effects of crystal diffraction and multiple scattering within reasonable approximations. Pierce et al⁶ recently measured the S - E curves from an amorphous ferromagnet $Fe_{40}Ni_{40}B_{20}$. These curves appear much simpler than those from a single crystal Fe surface and change sign only near 10 eV and 50 eV. Between these two energies S is negative, i.e., electrons polarized antiparallel to the sample spin are preferentially scattered. S is otherwise positive throughout the measured energy region (≤ 300 eV). Recently Nesbet⁷ proposed an electron resonance model to explain the change of sign near 50 eV. Namely, in Fe atom the electronic configuration is $3p^6 4s^2 3d^6$ and so long as two localized d-shell hole states are vacant, an electron incident on Fe with sufficient energy E^* for a $3p \rightarrow 3d$ excitation could be temporarily captured into a resonance state of Fe^- with configuration $3p^5 4s^2 3d^8$. Since the magnetic moment of Fe atom is $2 \mu_B$ (Bohr magneton), the resonance state could be a doublet (if the incident electron spin is '-') or quartet (if the incident electron spin is '+') depending on the polarization of the incident electron.

This results in two resonance energies E_D^* and E_Q^* separated by the Zeeman energy. At $E_D^*(E_Q^*)$, $I^-(I^+)$ is resonantly scattered and therefore $I^-(I^+) \gg I^+(I^-)$ and $S < 0$ ($S > 0$). Nesbet was able to explain that between E_D^* and E_Q^* S should go through zero and this occurs at ~ 50 eV. But the sign of S is left undiscussed. His model also can not explain the second zero at 10 eV observed experimentally. According to Hund's rule, the quartet energy is lower than the doublet energy. Therefore $E_Q^* < E_D^*$ and S should be positive just below 50 eV and negative just above 50 eV. But this is opposite to what has been observed experimentally. Also experimental data do not show any intensity enhancement due to resonance at ~ 50 eV. In fact the experimental intensity is near a minimum in this energy region⁶. We think that due to the limited spatial extent in a crystal-like environment, if F^- exists the life-time would be too short and the resonance would be too broad to be observed at all. It is the purpose of this letter to show that the electron kinematic scattering is the predominant mechanism for the elastic backward scattering of electrons from ferromagnetic $Fe_{40}Ni_{40}B_{20}$. The scattering asymmetry factors result mainly from the spin polarized exchange-correlation potentials and the glassy ferromagnetic materials are best suited to obtain a first insight into the single atom exchange scattering. We outline the details of our theory as follows:

Spin polarized atomic potentials for independent Fe and Ni atoms were generated by obtaining electron densities using Clementi's Hartree-Fock atomic wavefunctions and muffin-tin approximations. The net spin density was assumed to come from d electrons only. The boron atom was assumed spin unpolarized. Three different potentials have been constructed following Salter (K)⁸, Kohn-Sham (KS)⁹ and von Barth and Hedin (VH)¹⁰. All of them were derived by using local-spin-density (LSD) approximation and they differ in the treatment of the spin-dependent exchange-correlation potential. K

includes a momentum-dependent Slater exchange potential. KS includes a momentum-averaged exchange potential based on K and VH includes correlation energies in addition to KS. The VH potential reduces to the Hedin-Lundqvist potential in the paramagnetic limit. We calculated electron scattering phase shifts for electron angular momentum up to $\ell = 9$ and for energies up to 250 eV. The crystalline magnetic moments were used for Fe and Ni, namely 2.15 and 0.59 Bohr magneton (μ_B) per atom, respectively¹¹. This gives an effective magnetic moment of $1.1 \mu_B$ in comparison with the experimental value of $2.2 \mu_B$ per formula unit for the $\text{Fe}_{40}\text{Ni}_{40}\text{B}_{20}$ surface¹². We shall later propose an explanation for this difference. A spin-independent imaginary potential $V_i = 0.85 E^{1/3}$ (eV)¹³ was included to account for the energy dependence of the attenuation. The scattering geometry is shown in Fig. 1 in which α is the sample tilting angle and θ is the polar angle of the scattered intensity. The incident electron spin is made to lie within the scattering plane to minimize the effects of spin-orbit coupling. The scattering intensity at a specified angle θ is calculated by superimposing intensities due to each atomic scattering according to

$$I^{+(-)}(\theta) = \sum_j (e^{-M_j} |t_j^{+(-)}(\theta)|)^2 \times e^{-d/\lambda}, \quad (1)$$

where $j = \text{Fe, Ni or B}$ and e^{-M_j} is the Debye-Waller factor for atomic thermal vibrations, $t_j^{+(-)}(\theta)$ is the atomic scattering amplitude for incident electron beam having spin fully polarized parallel (+) or antiparallel (-) to the majority spin direction in the sample. $\lambda = \sqrt{2E}/(2V_i)$ is the electron mean-free path and $d = 1.66 (1/\cos\alpha + 1/\cos(\pi - (\alpha+\theta)))$ (in a.u.) is the distance that an electron travels through the crystal to scatter once with the first-layer surface atoms.

Contributions due to deeper layers can be neglected to a good approximation. 1.66 a.u. is the effective radius of each atom. We found that B is a much weaker scatterer than Fe and Ni and Fe is the main magnetic scatterer. Out of the three I-E curves calculated for $\alpha = 0^\circ$, $\theta = 166^\circ$, the Slater K-dependent potential produces a stronger energy dependence than the VH and KS potential and the VH potential produces results agree with the experimental curve⁶ the best. These curves are shown in Fig. 2.

We now proceed to the main point of this letter, namely the spin dependence S of the elastic scattering and particularly its dependence on the energy E of the electrons.

Figure 3 shows the result of the experiment together with theoretical single atom exchange scattering. The inner potential in the solid has been chosen as 14 eV for K, KS and VH respectively, such that in all curves the $S = 0$ points are fit to coincide at $E = 50$ eV (this shift also brings the major minimum in the I-E curve to coincide with the experimental minimum). We also show the S-E curve obtained by using Messmer's self-consistent field spin polarized X- α potential¹⁴ (M) from a $\text{Fe}_2\text{Ni}_2\text{B}$ cluster calculation. His effective magnetic moment is $1.38 \mu_B$ in good agreement with the measured bulk value $1.31 \mu_B$ ¹⁵. The shapes of the S-E curves of KS and M are very similar since the hybridized s, p, d spin densities due to the alloying effect in $\text{Fe}_2\text{Ni}_2\text{B}$ is mainly an interaction between Ni and B atoms and does not produce substantial changes in the Fe magnetic properties. All four curves show reasonable agreement with experimental results and clearly indicate that the spin dependent exchange-correlation interaction is the dominant mechanism for the intensity asymmetry. On the whole the VH potential gives the best agreement with experimental data in terms of peak positions and shapes. The K potential shows better results at higher energies due to the inclusion of energy dependence. However, since the experimental surface magnetic moment of $\text{Fe}_{40}\text{Ni}_{40}\text{B}_{20}$ ⁶ is about

twice the theoretical values^{11,14} and the experimental bulk values¹⁵, the experimental S values also shows about a factor of 2 difference with theory. The experimental magnetic moments of $\text{Fe}_{40}\text{Ni}_{40}\text{B}_{20}$, $\text{Fe}_{80}\text{B}_{20}$ and $\text{Fe}_{81.5}\text{B}_{14.5}\text{Si}_4$ ⁶ are all about the same. This leads us to think that the first layer of $\text{Fe}_{40}\text{Ni}_{40}\text{B}_{20}$ surface could be predominantly composed of Fe atoms.

Below 30 eV current theoretical results do not agree with experimental data even allowing for the spin dependence in the imaginary potential as proposed by Feder ($V_F^{+(-)}$)¹⁶ and Rendell and Penn ($V_{RP}^{+(-)}$)¹⁷. Since $V_F^{(-)}$ is always larger than $V_F^{(+)}$, the inclusion of them will raise the S values throughout the energy range and makes no improvement for $E \leq 30$ eV. On the other hand $V_{RP}^{(-)}$ is smaller than $V_{RP}^{(+)}$ for Fe at $E \leq 95$ eV, which will lower the S values. Unfortunately, the absolute values of $V_{RP}^{+(-)}$ are so small at these low energies that they cannot compete with the spin dependent elastic scattering strength.

In summary, this work presents the dominant mechanism for intensity asymmetries observed in spin polarized low energy electron scattering by amorphous magnetic surfaces and points out the error of the recently proposed resonance model. Theoretically this work also presents the first results of spin polarized electron scattering calculations by atoms using potentials derived from LSD formalism. Since intensity asymmetry is much more sensitive to the details of the potential than the intensity itself is, such calculations present a challenge to the current spin polarized exchange-correlation potential models for the calculation of continuum wavefunctions especially at the very low energies. We hope that our results will stimulate further research in this direction.

References

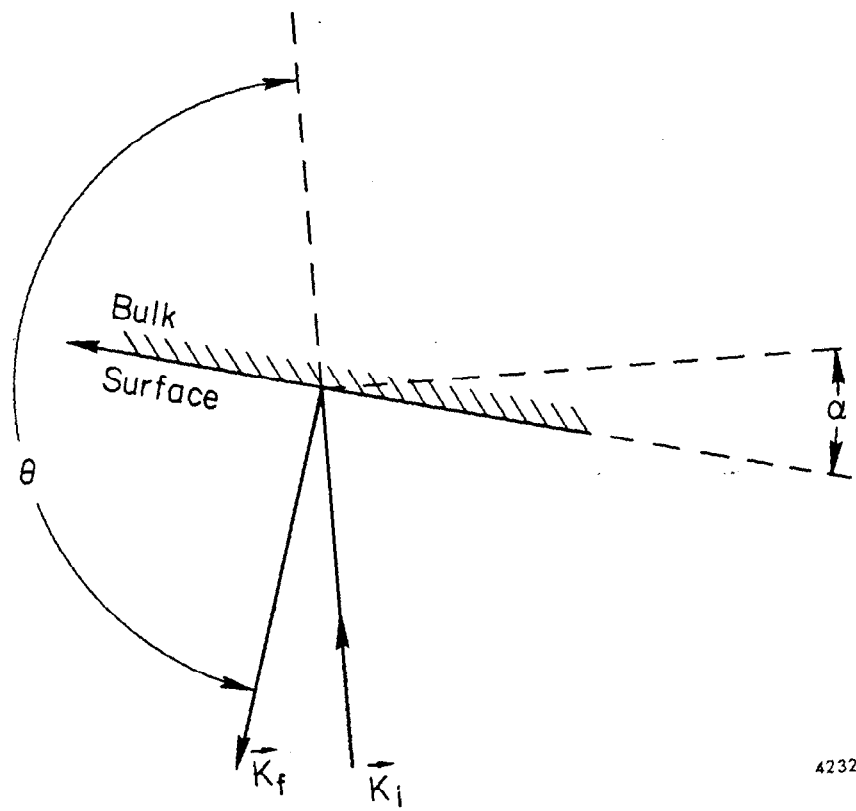
1. R. J. Celotta, D. T. Pierce, G.-C. Wang, S. D. Bader, and G. P. Felder, Phys. Rev. Lett. 43, 728 (1979).
2. S. W. Wang, R. E. Kirby, and E. L. Garwin, Solid State Commun., 32, 993 (1979).
3. S. W. Wang, Solid State Commun., 36, 847 (1980).
4. D. T. Pierce and R. J. Celotta, Adv. Electronics and Electron Physics, 56, 219 (1981).
5. J. S. Schilling and M. B. Webb, Phys. Rev. B, 2, 1665 (1970).
6. D. T. Pierce, R. J. Celotta, H. C. Siegmann, and J. Unguris, submitted to Physical Review B.
7. R. K. Nesbet, submitted to Physical Review Letters.
8. J. C. Slater, Phys. Rev., 179, 28 (1969); Phys. Rev., 165, 658 (1968).
9. W. Kohn and L. J. Sham, Phys. Rev., 140, A1133 (1965).
10. U. VonBarth and L. Hedin, J. Phys. C5, 1629 (1972); see also ref. 11, p. 15-16, eq. (2.5)-(2.9).
11. V. L. Moruzzi, J. F. Janak, and A. R. Williams, "Calculated Electronic Properties of Metals", Pergamon, New York (1978).
12. H. C. Siegmann, D. T. Pierce and R. J. Celotta, Phys. Rev. Lett., 46, 452 (1981).
13. For a review, see J. B. Pendry, "Low Energy Electron Diffraction", Academic Press, London and New York (1974).
14. R. P. Messmer, Phys. Rev. B23, 1616 (1981).
15. J. J. Becker, F. E. Luborsky, and J. L. Walter, IEEE Trans. Magn. MAG-13, 988 (1977).
16. R. Feder, Solid State Commun., 31, 821 (1979).
17. R. W. Rendell and D. R. Penn, Phys. Rev. Lett., 45, 2057 (1980).

Figure Captions

Figure 1: Scattering geometry. α denotes inclination angle of the sample with respect to the incident electron beam. The direction of magnetization in $\text{Fe}_{40}\text{Ni}_{40}\text{B}_{20}$ is indicated by an arrow. θ is the scattering polar angle with respect to the incident direction.

Figure 2: Experimental and theoretical elastically scattered intensity vs incident electron energy at $\alpha = 0^\circ$ and $\theta = 166^\circ$.

Figure 3: The experimental and theoretical S-E curves for electrons scattered elastically in the backward direction ($\theta = 166^\circ$) and $\alpha = 0^\circ$ for $\text{Fe}_{40}\text{Ni}_{40}\text{B}_{20}$ at room temperature. VH uses von Barth and Hedin's spin polarized exchange-correlation potential, KS the Kohn-Sham potential, M uses the Messmer SCF- X_α potential, and K uses Slater's k-dependent exchange potential, see Ref. 8, 9, 10, 14 respectively. The experimental results were taken from ref. 4.



11-81

4232A1

Fig. 1

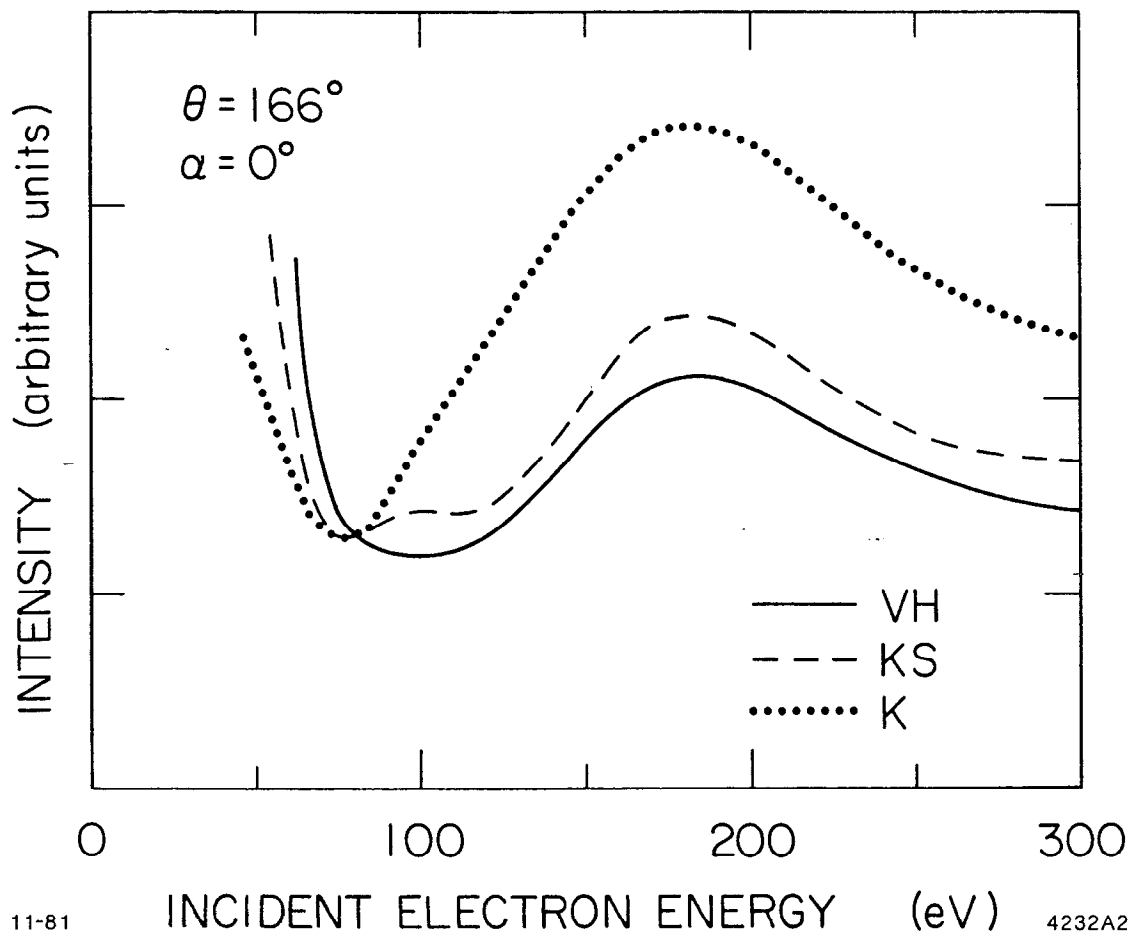


Fig. 2

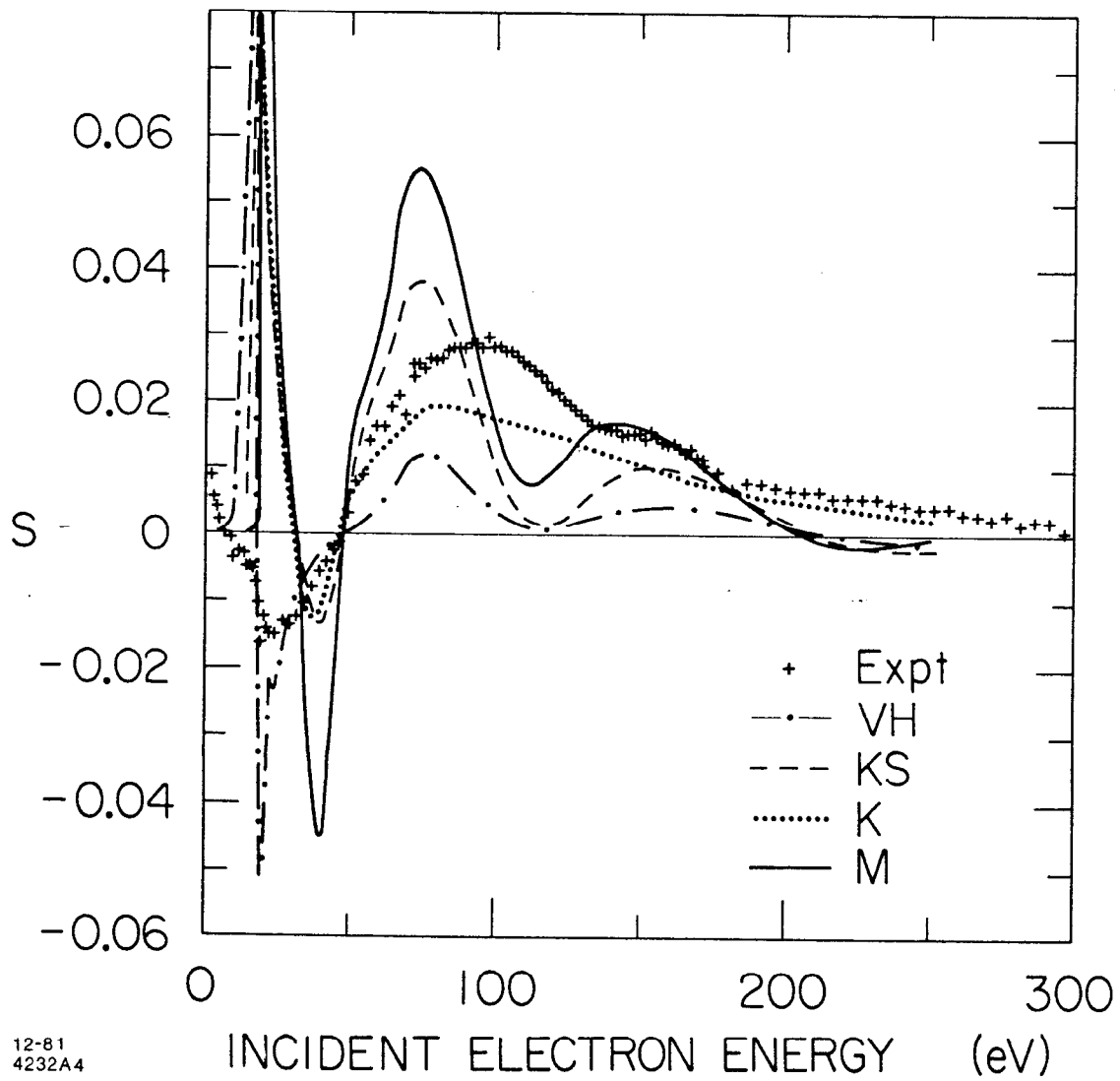


Fig. 3